A study of O 2 (a 1 Δ g) with photoelectron spectroscopy using synchrotron radiation

Jonathan D. Barr, Alberto De Fanis, John M. Dyke, Stuart D. Gamblin, Alan Morris, Stefano Stranges, John B. West, Timothy G. Wright, and Andrew E. Wright

Citation: The Journal of Chemical Physics **109**, 2737 (1998); doi: 10.1063/1.476872
View online: http://dx.doi.org/10.1063/1.476872
View Table of Contents: http://scitation.aip.org/content/aip/journal/jcp/109/7?ver=pdfcov
Published by the AIP Publishing

A study of $O_2(a\ ^1\Delta_g)$ with photoelectron spectroscopy using synchrotron radiation

Jonathan D. Barr, Alberto De Fanis, John M. Dyke,[a] Stuart D. Gamblin, Alan Morris, Stefano Stranges,[b] John B. West,[c] Timothy G. Wright, and Andrew E. Wright
Department of Chemistry, University of Southampton, Highfield, Southampton SO17 1BJ, United Kingdom

(Received 18 March 1998; accepted 14 May 1998)

The atmospherically important species $O_2(a\ ^1\Delta_g)$ has been studied by photoelectron spectroscopy using vacuum ultraviolet radiation from a synchrotron as the photon source. Constant-ionic-state (CIS) spectra, recorded for vibrational levels of $O_2^+(X\ ^2\Pi_g)$ $v^+=0,1,2,3$ accessed from $O_2(a\ ^1\Delta_g)$ $v''=0$, exhibit intense signals in the photon energy region 14.0–15.5 eV which are shown to arise from autoionization from a Rydberg state with an $O_2^+(C\ ^2\Phi_u)$ core. On the basis of the results obtained and earlier evidence derived from vacuum ultraviolet absorption spectroscopy, this state is assigned as a $(C\ ^2\Phi_u,3s\sigma_g)\ ^1\Phi_u$ Rydberg state. Photoelectron spectra recorded for $O_2(a\ ^1\Delta_g)$ at positions of strong resonances have allowed extended vibrational structure to be obtained in the first photoelectron band. The relative vibrational component intensities in the resonant photoelectron spectra are in good agreement with computed relative intensities obtained via Franck–Condon calculations, confirming the vibrational numbering of the resonances in the $^1\Phi_u$ state. Competition between autoionization and predissociation in the $^1\Phi_u$ Rydberg state is discussed on the basis of the results obtained. Weaker structure is observed in CIS spectra recorded in the photon energy regions 12.5–13.5 and 15.0–20.0 eV. Suggestions are made for the nature of the highly excited states of O_2 associated with this structure, based on available ionization energies and spectroscopic constants of known ionic states accessible from $O_2(a\ ^1\Delta_g)$. For example, two broad bands centered at ≈16.4 and ≈17.75 eV are assigned to excitation to Rydberg states arising from the configurations $(D\ ^2\Delta_g,3p\pi_u)$ and $(D\ ^2\Delta_g,4p\pi_u)$, respectively. © *1998 American Institute of Physics.* [S0021-9606(98)01631-6]

I. INTRODUCTION

As oxygen is a major atmospheric constituent, vacuum ultraviolet photoionization of O_2, a process which occurs in the upper atmosphere with solar radiation, has been the subject of extensive investigations by photoionization mass spectrometry[1] and photoelectron spectroscopy.[2–7] The first excited state of oxygen, the $a\ ^1\Delta_g$ state, is also an important atmospheric component. It is present in relatively high partial pressures in the troposphere, being produced with $O(^1D)$ from photolysis of ozone, and is one of the strongest contributors to the atmospheric airglow.[8] Photoionization of $O_2(a\ ^1\Delta_g)$ has been suggested as an important source of ions in the D region of the atmosphere to explain both the O_2^+ partial pressures and the total ion densities at these altitudes.[9–11] $O_2(a\ ^1\Delta_g)$ ionization is also thought to be important at lower altitudes (<70 km) in providing a source of O_2^+ which can be involved, with NO, NO^+, and H_2O, in a sequence of reactions leading to the formation of protonated water clusters.[12,13]

The ground electronic configuration of O_2, which gives rise to the X, a, and b states, is

$$1\sigma_g^2\ 1\sigma_u^2\ 2\sigma_g^2\ 2\sigma_u^2\ 3\sigma_g^2\ 1\pi_u^4\ 1\pi_g^2.$$

In the HeI photoelectron spectrum of $O_2(X\ ^3\Sigma_g^-)$ five bands are observed,[2] corresponding to ionization to the O_2^+ states $X\ ^2\Pi_g$, $a\ ^4\Pi_u$, $A\ ^2\Pi_u$, $b\ ^4\Sigma_g^-$, and $B\ ^2\Sigma_g^-$ with respective adiabatic ionization energies of 12.07, 16.10, 17.04, 18.17, and 20.30 eV. Removal of the $1\pi_g$ electron gives the $X\ ^2\Pi_g$ state of O_2^+, removal of the $1\pi_u$ electron gives the $a\ ^4\Pi_u$ and $A\ ^2\Pi_u$ ionic states, and the $b\ ^4\Sigma_g^-$ and $B\ ^2\Sigma_g^-$ states arise from removal of a $3\sigma_g$ electron. For $O_2(a\ ^1\Delta_g)$, electron removal from the $1\pi_g$ level gives $O_2^+(X\ ^2\Pi_g)$, while loss of an electron from the $1\pi_u$ level gives $O_2^+(C\ ^2\Phi_u)$ and $(A\ ^2\Pi_u)$ and the $(3\sigma_g)^{-1}$ ionization gives $O_2^+(D\ ^2\Delta_g)$. By recording a HeI photoelectron spectrum of discharged oxygen, and subtracting a spectrum recorded with the discharge off, well-resolved photoelectron bands have been recorded for the ionizations $O_2^+(X\ ^2\Pi_g)\leftarrow O_2(a\ ^1\Delta_g)$, $O_2^+(A\ ^2\Pi_u)\leftarrow O_2(a\ ^1\Delta_g)$, $O_2^+(C\ ^2\Phi_u)\leftarrow O_2(a\ ^1\Delta_g)$, and $O_2^+(D\ ^2\Delta_g)\leftarrow O_2(a\ ^1\Delta_g)$.[14,15]

Rydberg excited states of $O_2(a\ ^1\Delta_g)$ which are members of series which converge to the first ionic state, $O_2^+(X\ ^2\Pi_g)$, have been studied in some detail by laser multiphoton ionization spectroscopy.[16–21] Also, the photoionization cross section of $O_2(a\ ^1\Delta_g)$ has been measured between the ionization thresholds of the a and the X neutral states (11.09–12.07 eV).[22] Some resonant structure was observed in the photoionization efficiency curves obtained, but no excited state

[a]Author to whom correspondence should be addressed.
[b]Department of Chemistry, ''La Sapienza,'' University of Rome, Italy.
[c]CLRC, SR Department, Daresbury Laboratory, Daresbury, Warrington, Cheshire, WA4 4AD, UK.

assignments were made. This excitation energy range is calculated to be too low for the observation of Rydberg states which are parts of series converging to $O_2^+(A\ ^2\Pi_u)$, the lowest accessible excited state of O_2^+, so these resonant features probably correspond to vibrational autoionization from Rydberg states with an $O_2^+(X\ ^2\Pi_g)$ core or autoionization from an excited state of valence character. Measurements of the absorption spectrum of $O_2(a\ ^1\Delta_g)$ in the energy region 7.5–11.1 eV revealed excitation to Rydberg states which are parts of series converging to $O_2^+(X\ ^2\Pi_g)$.[23] In this investigation strong $np\pi$ and weak $np\sigma$ series were observed, in addition to a series tentatively assigned to excitation to nf orbitals.[23] Absorption spectra of $O_2(a\ ^1\Delta_g)$ in the energy regions 7.6–9.6 and 13.7–14.8 eV have been observed by Katayama, Huffman, and co-workers.[24–26] In the earlier studies,[24,25] a vibrationally resolved band at ≈14.0 eV excitation energy was assigned to a $(C\ ^2\Phi_u,3s\sigma_g)\ ^1\Phi_u \leftarrow a^1\Delta_g$ transition. Some of the vibrational components were rotationally resolved and an unusual alternating pattern of narrow and broad lines was observed in the vibrational members of this band, which was attributed to a combination of predissociation and autoionization. In the third study,[26] at lower excitation energy, an absorption of $O_2(b\ ^1\Sigma_g^+)$ was observed, and some other, diffuse features were assigned to $O_2(a\ ^1\Delta_g)$ absorptions.

The objective of the present work was to obtain more information on Rydberg states of $O_2(a\ ^1\Delta_g)$ which lie above the first ionization threshold and to record photoelectron spectra at resonant photon energies, with the aim of obtaining extended vibrational structure, particularly in the first photoelectron band, as has been done previously for SO (Ref. 27) and CS (Ref. 28).

II. EXPERIMENT

The photoelectron spectrometer built for this project was designed for use with the UK synchrotron radiation source (SRS) located at Daresbury Laboratory.

The synchrotron radiation was dispersed by a 5 m normal incidence McPherson monochromator before it entered the spectrometer. This consisted of an ionization chamber, a three element lens assembly, a 10 cm mean radius hemispherical electrostatic analyzer, and a channeltron detector.[27,28] The photoelectron resolution achieved at 5 eV pass energy was typically 40 meV.

Experiments could be performed either of the conventional photoelectron spectroscopy (PES) type, in which photoelectron spectra are recorded at a fixed photon energy, or of the constant-ionic-state (CIS) type in which the intensity of a particular photoelectron feature (such as a vibrational component in a photoelectron band) is monitored as a function of photon energy.

$O_2(a\ ^1\Delta_g)$ was produced by passing oxygen through a microwave discharge (2.45 GHz) in a glass inlet tube attached to the ionization chamber. The discharge products were then pumped rapidly through the ionization chamber of the spectrometer. It is known that $O_2(a\ ^1\Delta_g)$ is the dominant excited molecular product from such a discharge along with atomic oxygen and negligible amounts of $O_2(b\ ^1\Sigma_g^+)$.[14] From published HeI photoionization cross sections of the $a\ ^1\Delta_g$ and $X\ ^3\Sigma_g^-$ states of O_2,[29] and the relative intensities observed in HeI photoelectron spectra recorded for a typical discharge, the yield of $O_2(a\ ^1\Delta_g)$ produced by the discharge is estimated to be ≈15%.

The synchrotron photon energy was calibrated by recording the CIS spectrum of $O(^3P)$ in the photon energy region 13.5–19.0 eV and comparing the positions of the O* resonances, which autoionize to $O^+(^3P)$, with those known in the literature.[30]

III. RESULTS AND DISCUSSION

A HeI photoelectron spectrum recorded for an oxygen discharge is shown in Fig. 1, with the assignment of the major features indicated in the caption. The 0.98 eV excitation energy of $O_2(a\ ^1\Delta_g)$ relative to $O_2(X\ ^3\Sigma_g^-)$ means that the first four vibrational components of the $O_2^+(X\ ^2\Pi_g) \leftarrow O_2(a\ ^1\Delta_g)$ band (labeled 1 in Figure 1) are observed before the onset of the more intense $O_2^+(X\ ^2\Pi_g) \leftarrow O_2(X\ ^3\Sigma_g^-)$ band (labeled 2 in Fig. 1). Also observed are features due to oxygen atoms, labeled as 3 and 5. The second and third bands of $O_2(a\ ^1\Delta_g)$, arising from ionization to the $A\ ^2\Pi_u$ and $C\ ^2\Phi_u$ ionic states, occur in the regions labeled 4 and 6 in Fig. 1. These bands are not resolved in Fig. 1, but can be clearly observed if the discharge is pulsed and a phase-sensitive method is used to detect photoelectron signals in-phase and out-of-phase with the discharge.[14,15,31] A photoelectron spectrum recorded with this method is shown in Fig. 2 where signals due to $O_2(X\ ^3\Sigma_g^-)$ are observed out-of-phase with the discharge (below the baseline in Fig. 2) whereas those due to $O(^3P)$ and $O_2(a\ ^1\Delta_g)$ are observed in-phase with the discharge (above the baseline in Fig. 2). The $O_2^+(A\ ^2\Pi_u) \leftarrow O_2(a\ ^1\Delta_g)$ and the $O_2^+(C\ ^2\Phi_u) \leftarrow O_2(a\ ^1\Delta_g)$ bands can be clearly seen in this figure. The measured separations in these vibrationally resolved bands gave $\omega_e = (898 \pm 30)\ \mathrm{cm}^{-1}$ and $\omega_e x_e = (14 \pm 5)\ \mathrm{cm}^{-1}$, $\omega_e = (1043 \pm 26)\ \mathrm{cm}^{-1}$ and $\omega_e x_e = (9 \pm 4)\ \mathrm{cm}^{-1}$ in the $A\ ^2\Pi_u$ and $C\ ^2\Phi_u$ ionic states, respectively.[14,15,31]

As the first four vibrational components of the $O_2^+(X\ ^2\Pi_g)$, $v^+ \leftarrow O_2(a\ ^1\Delta_g)$, $v''=0$ band do not overlap with the $O_2^+(X\ ^2\Pi_g)$, $v^+ \leftarrow O_2(X\ ^3\Sigma_g^-)$, $v''=0$ photoelectron band, CIS spectra can readily be recorded for these first four components of the first $O_2(a\ ^1\Delta_g)$ photoelectron band. The CIS spectrum for $O_2^+(X\ ^2\Pi_g)$, $v^+=2 \leftarrow O_2(a\ ^1\Delta_g)$, $v''=0$, recorded over the photon energy range 12.0–20.0 eV, is shown in Fig. 3. Very low signals were observed between the ionization threshold (≈11.55 eV for $v^+=2$) and 12.0 eV because of low photon flux. The strongest features in Fig. 3 are two intense bands in the 14.0–15.0 eV region. Other signals were observed, notably weak features between 12.5 and 13.5 eV, a stronger, broad structured band at ≈16.0 eV and weaker features centered at approximately 18.5 eV. This CIS spectrum will be considered in three sections, (A): 14.0–15.5 eV, (B): 12.5–13.5 eV, and (C): 15.5–19.0 eV.

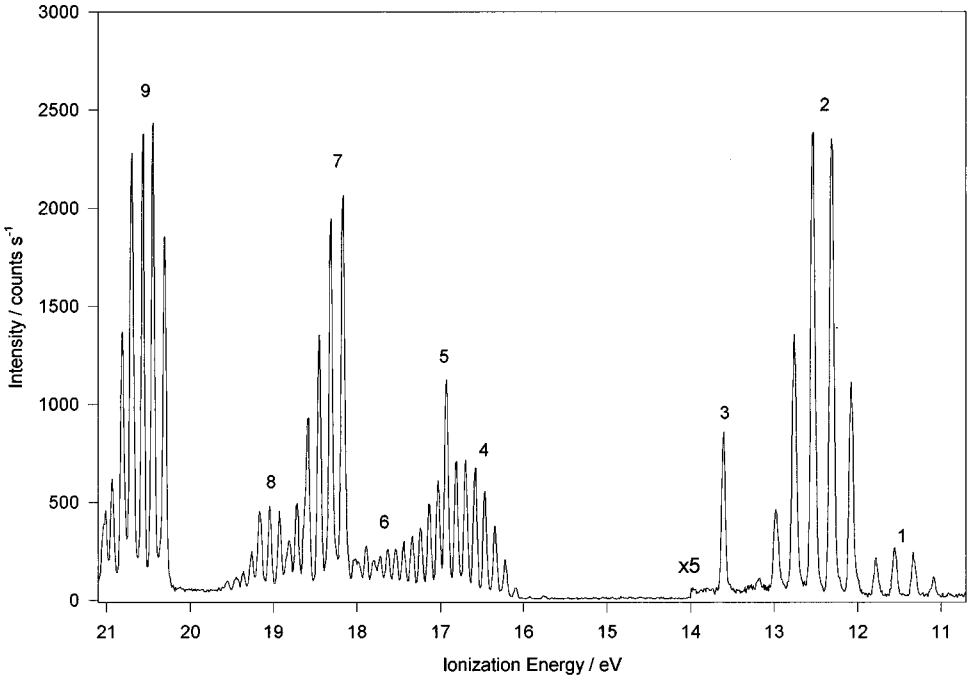

FIG. 1. HeI photoelectron spectrum recorded for discharged oxygen. In this figure, numbers are used as follows to label bands associated with the following ionizations
1. $O_2^+(X\ ^2\Pi_g) \leftarrow O_2(a\ ^1\Delta_g)$;
2. $O_2^+(X\ ^2\Pi_g) \leftarrow O_2(X^3\Sigma_g^-)$;
3. $O^+(^4S) \leftarrow O(^3P)$;
4. $O_2^+(a\ ^4\Pi_u) \leftarrow O_2(X\ ^3\Sigma_g^-)$;
   $O_2^+(A\ ^2\Pi_u) \leftarrow O_2(a\ ^1\Delta_g)$;
5. $O^+(^2D) \leftarrow O(^3P)$;
6. $O_2^+(A\ ^2\Pi_u) \leftarrow O_2 \times (X\ ^3\Sigma_g^-)$;
   $O_2^+(C\ ^2\Phi_u) \leftarrow O_2(a\ ^1\Delta_g)$;
7. $O_2^+(b\ ^4\Sigma_g^-) \leftarrow O_2(X\ ^3\Sigma_g^-)$;
8. $O_2^+(D\ ^2\Delta_g) \leftarrow O_2(a\ ^1\Delta_g)$;
9. $O_2^+(B\ ^2\Sigma_g^-) \leftarrow O_2(X\ ^3\Sigma_g^-)$.

A. $O_2^+(X\ ^2\Pi_g)$, $v^+ \leftarrow O_2(a\ ^1\Delta_g)$ $v''=0$ CIS spectra recorded in the photon energy region 14.0–15.5 eV

CIS spectra in this photon energy range have been recorded for the first four vibrational components of $O_2^+(X\ ^2\Pi_g)$ and are shown in Fig. 4. Each spectrum has been corrected for variation in photon flux. Two bands, labeled *A* and *B*, dominate the spectra at 14.11 and 14.37 eV. It was not immediately obvious why only two intense bands were observed; they are approximately 2100 cm^{-1} apart, roughly twice the vibrational separation of any known excited state of O_2^+, so they cannot represent consecutive vibrational levels in a Rydberg state. The intensities of these bands are unusually high and photoelectron spectra recorded at these photon energies (shown later) demonstrate that these photon energies correspond to autoionization resonances of $O_2(a\ ^1\Delta_g)$. The first two excited states of O_2^+ accessible from $O_2(a\ ^1\Delta_g)$ are the $O_2^+(A\ ^2\Pi_u)$ and $O_2^+(C\ ^2\Phi_u)$ states, with adiabatic ionization energies of 16.06 and 17.51 eV, respectively.[14,15,31] Hence the possibility that bands *A* and *B* are components of a Rydberg state with an $O_2^+(A\ ^2\Pi_u)$ or an $O_2^+(C\ ^2\Phi_u)$ core was investigated initially, although it was noted that the *A*-*B* separation in Fig. 4 was too large to be two vibrational separations in a Rydberg state with an $O_2^+(A\ ^2\Pi_u)$ core.

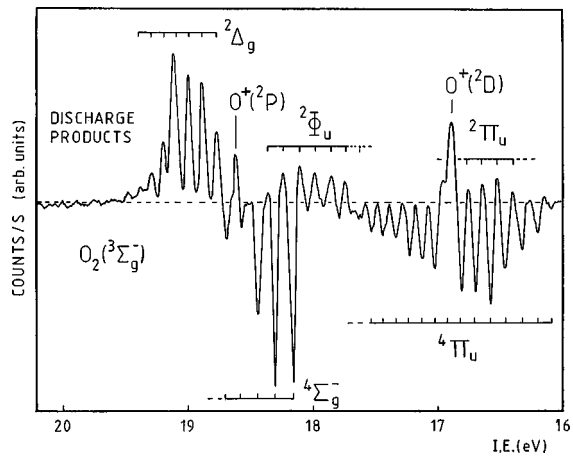

FIG. 2. Phase-sensitive detection HeI photoelectron spectrum recorded for discharged oxygen. The discharge is pulsed and a phase sensitive detection method is used. Features above the horizontal baseline are in-phase with the discharge and features below are out-of-phase with the discharge. Hence the features above the baseline correspond to discharge products.

As mentioned earlier, Katayama, Huffman, and co-workers[24,25] have observed absorption to an excited state of $O_2(a\ ^1\Delta_g)$ in this photon energy region. In the experimental vacuum ultraviolet (vuv) absorption spectrum[24] not all vibrational levels in the excited state were observed and only a few vibronic bands were rotationally resolved. Analysis of the absorption spectrum yielded upper state constants of $\omega_e' = 1071 \pm 4\ cm^{-1}$, $\omega_e x_e' = 8.3 \pm 0.8\ cm^{-1}$, and $r_e' = 1.374 \pm 0.008$ Å,[24] values which are sufficiently similar to the known constants of $O_2^+(C\ ^2\Phi_u)$, derived from analysis of the vibrationally resolved $O_2^+(C\ ^2\Phi_u) \leftarrow O_2(a\ ^1\Delta_g)$ photoelectron band, to imply Rydberg character for the excited state with an $O_2^+(C\ ^2\Phi_u)$ core. The $v'=0$ band occurs at 13.74 eV excitation energy which, when combined with the known adiabatic ionization energy (AIE) for $O_2^+(C\ ^2\Phi_u) \leftarrow O_2(a\ ^1\Delta_g)$ of 17.51 eV, gives an effective principal quantum number, n^*, of 1.90.[24] This is consistent with $n=3$, $\delta = 1.10$ (where δ is the quantum de fect) implying an outermost 3*s* Rydberg electron in the excited state.[32] The excited state is therefore labeled $(C\ ^2\Phi_u, 3s\sigma_g)\ p\ ^1\Phi_u$ (the *p* label comes from the tables of Ref. 33). This assignment implies that bands *A* and *B* correspond to excitation to $v'=3$ and $v'=5$ in the $p\ ^1\Phi_u$ excited state. Closer inspection of Fig. 4 shows that a weak transition to $v'=7$ can be seen in some of the spectra.

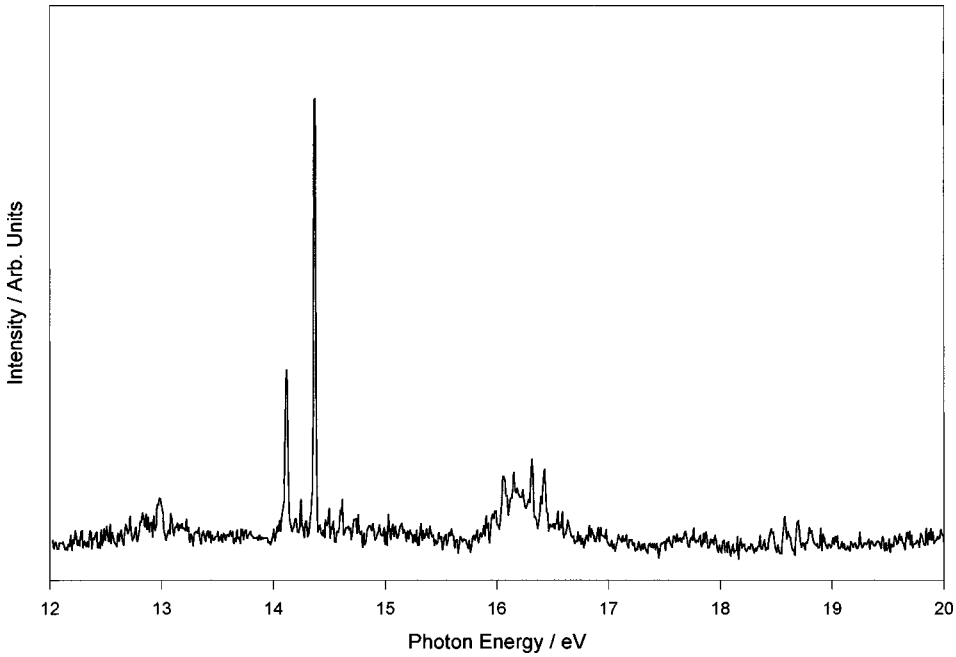

FIG. 3. CIS spectrum recorded for $O_2^+(X\ ^2\Pi_g)v^+=2\leftarrow O_2(a\ ^1\Delta_g)$, $v''=0$ over the photon energy region 12.0–20.0 eV.

An unusual feature of the vuv absorption band is that the vibrational components appear alternately sharp and diffuse.[24] Katayama *et al.* attribute this broadening to a combination of predissociation and autoionization in the vibrational levels in the excited $^1\Phi_u$ state.[24] The excitation energy at the band head and the appearance of each observed vibronic band of the $p\ ^1\Phi_u\leftarrow a\ ^1\Delta_g$ absorption taken from Ref. 24 are summarized in Table I and these band head positions are marked as vertical dotted lines in Fig. 4.

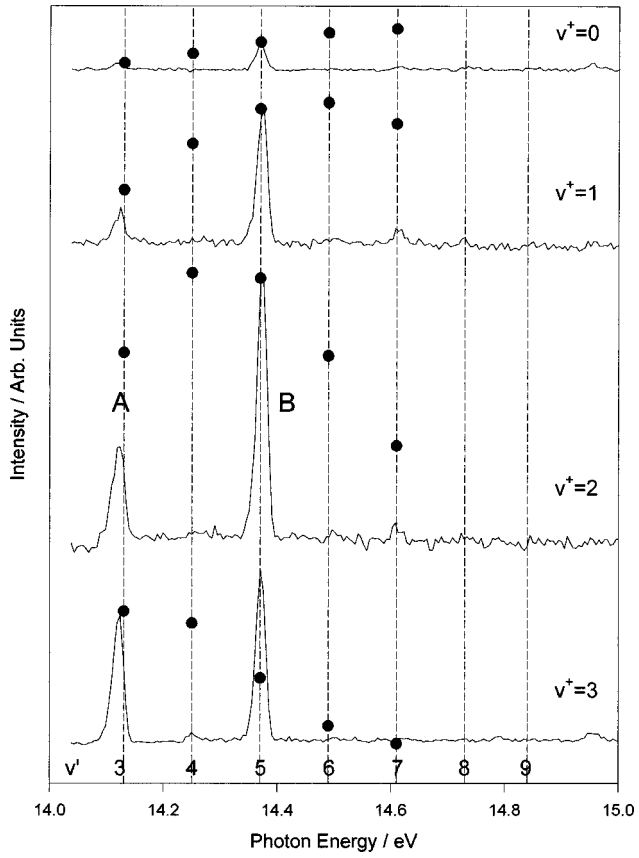

FIG. 4. CIS spectra recorded for $O_2^+(X\ ^2\Pi_g)v^+\leftarrow O_2(a\ ^1\Delta_g)v''=0$ over the photon energy region 14.0–15.0 eV, for $v^+=0$, 1, 2, 3. The black circles indicate the computed CIS relative intensities derived from Franck–Condon calculations (see the text).

As outlined previously,[27,28] if CIS spectra only arise from autoionization processes then it is expected that they can be simulated using a product of Franck–Condon factors for the two steps involved, i.e., (a) and (b) in

$$O_2(X\ ^2\Pi_g)v^+\overset{b}{\leftarrow}O_2^*,\quad v'\overset{a}{\leftarrow}O_2(a\ ^1\Delta_g)v''=0,$$

where O_2^* is a Rydberg state with an $O_2^+(C\ ^2\Phi_u)$ core. In these calculations each state is represented by a Morse potential specified using established values of r_e, ω_e, and $\omega_e x_e$ for $O_2(a\ ^1\Delta_g)$ and $O_2^+(X\ ^2\Pi_g)$ (Ref. 33) and the corresponding values for $O_2(p\ ^1\Phi_u)$ from the vuv absorption study.[24] Franck–Condon factors were computed for (a) and (b) for a range of v' values (e.g., $v'=0-10$) and a selected value of v^+ and simulated CIS spectra were derived by multiplying the two Franck–Condon factors together. The results obtained are shown as the solid black circles in Fig. 4. As

TABLE I. Summary of bandhead positions (E_{head}) and appearance of vibrational components in the $O_2(p\ ^1\Phi_u)v'\leftarrow O_2(a\ ^1\Delta_g)$. $v''=0$ absorption band (from Ref. 24).

v'	E_{head} /eV	Appearance
0	⋯	overlapped
1	13.87	overlapped
2	14.00	overlapped, diffuse
3	14.13	well rotationally resolved
4	14.25	diffuse
5	14.37	well rotationally resolved
6	14.49	diffuse
7	14.61	reasonably well rotationally resolved
8	14.73	poorly resolved
9	14.84	diffuse

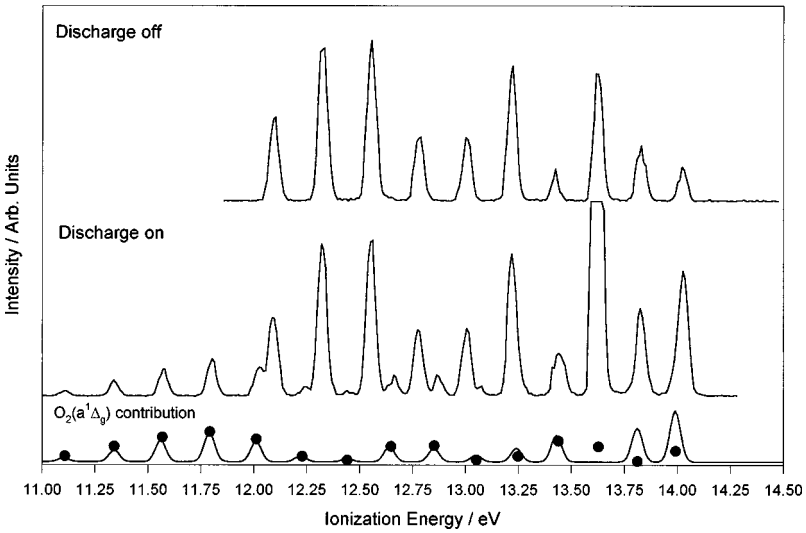

FIG. 5. Photoelectron spectra recorded at $h\nu = 14.11$ eV (i.e., at the position of band *A* in Fig. 4) for discharged and undischarged oxygen, in the ionization energy region 11.0–14.1 eV. The black circles in the lower part of this figure represent relative vibrational intensities obtained by summing the direct and autoionization computed envelopes (see the text).

can be seen, the fit between experimental and computed relative intensities is poor. However, for the two clearly observed bands *A* and *B*, the overall trend is correct with the intensity of *A* rising with respect to *B* as v^+ increases. This poor agreement is probably a consequence of competition between autoionization and predissociation in the excited $p^1\Phi_u$ state; if the $v'=3$ level is predissociated slightly more efficiently than $v'=5$ then the intensity of the $v'=3$ level will be lower than calculated, as is observed. Indeed, in the vuv absorption spectrum,[24] the $v'=3$ absorption band is slightly less well resolved than the $v'=5$ band and from the rotational linewidths in the absorption spectrum approximate lifetimes of the $v'=3$ and $v'=5$ levels may be estimated, after allowance for the instrumental contribution, as 1.8 and 2.6 ps, respectively. If it is assumed that predissociation of the $v'=5$ level is minimal, then 2.6 ps must represent the autoionization lifetime of this level. Predissociation of the $v'=3$ and 5 levels is presumably relatively slow while for the other vibrational levels it is much faster as little or no signals are seen for these levels in the CIS spectrum.

Photoelectron spectra of discharged oxygen recorded at photon energies corresponding to bands *A* and *B* in Fig. 4 (14.11 and 14.37 eV) are shown in Figs. 5 and 6, respectively. In each case comparison with spectra recorded with the discharge off allowed contributions from $O_2(a\ ^1\Delta_g)$ and $O(^3P)$ to the discharged oxygen spectrum to be identified. Since in both Figs. 5 and 6 some of the photoelectron signals arising from ionization of $O_2(a\ ^1\Delta_g)$ are partly obscured by stronger signals arising from $O_2(X\ ^3\Sigma_g^-)$, a program has been used to deconvolute and remove the $O_2(X\ ^3\Sigma_g^-)$ features from a spectrum recorded with the discharge on. The lowest trace in each figure shows the contribution from $O_2(a\ ^1\Delta_g)$, which represents the photoelectron spectrum of $O_2(a\ ^1\Delta_g)$ at the two photon energies used over the ionization energy region 11.0–14.5 eV, except between 13.5 and 13.7 eV ionization energy where contributions from molecular and atomic oxygen overlap, making accurate deconvolution impossible. [The $O^+(^4S) \leftarrow O(^3P)$ ionization occurs at 13.61 eV.[30]] The spectra recorded at these photon energies with the discharge off [i.e., for the $O_2(X\ ^3\Sigma_g^-)$ first band] show extra vibrational structure compared with the band envelope recorded with HeI radiation. Also, instead of showing four vibrational components for the $O_2^+(X\ ^2\Pi_g) \leftarrow O_2(a\ ^1\Delta_g)$ ionization, as are observed in the HeI (21.22 eV) photoelectron spectrum, 16 components are observed.

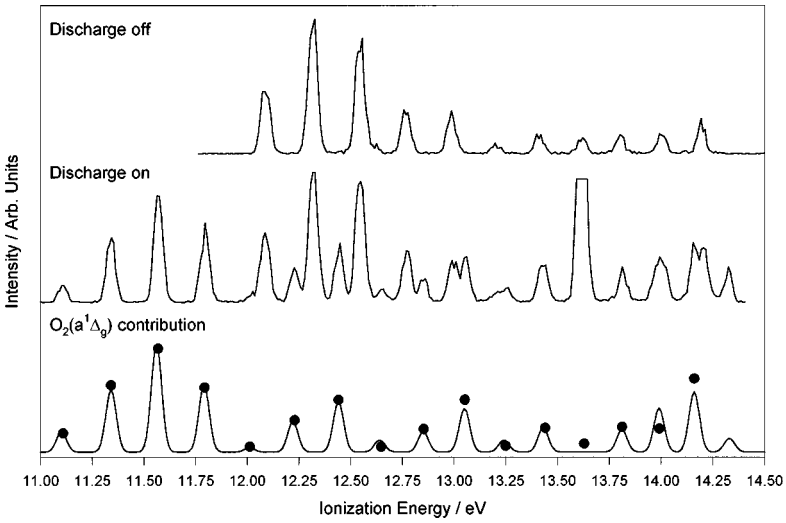

FIG. 6. Photoelectron spectra recorded at $h\nu = 14.37$ eV (i.e., at the position of band *B* in Fig. 4) for discharged and undischarged oxygen, in the ionization energy region 11.0–14.4 eV. The black circles in the lower part of this figure represent computed relative vibrational intensities obtained by summing the direct and autoionization computed envelopes (see the text).

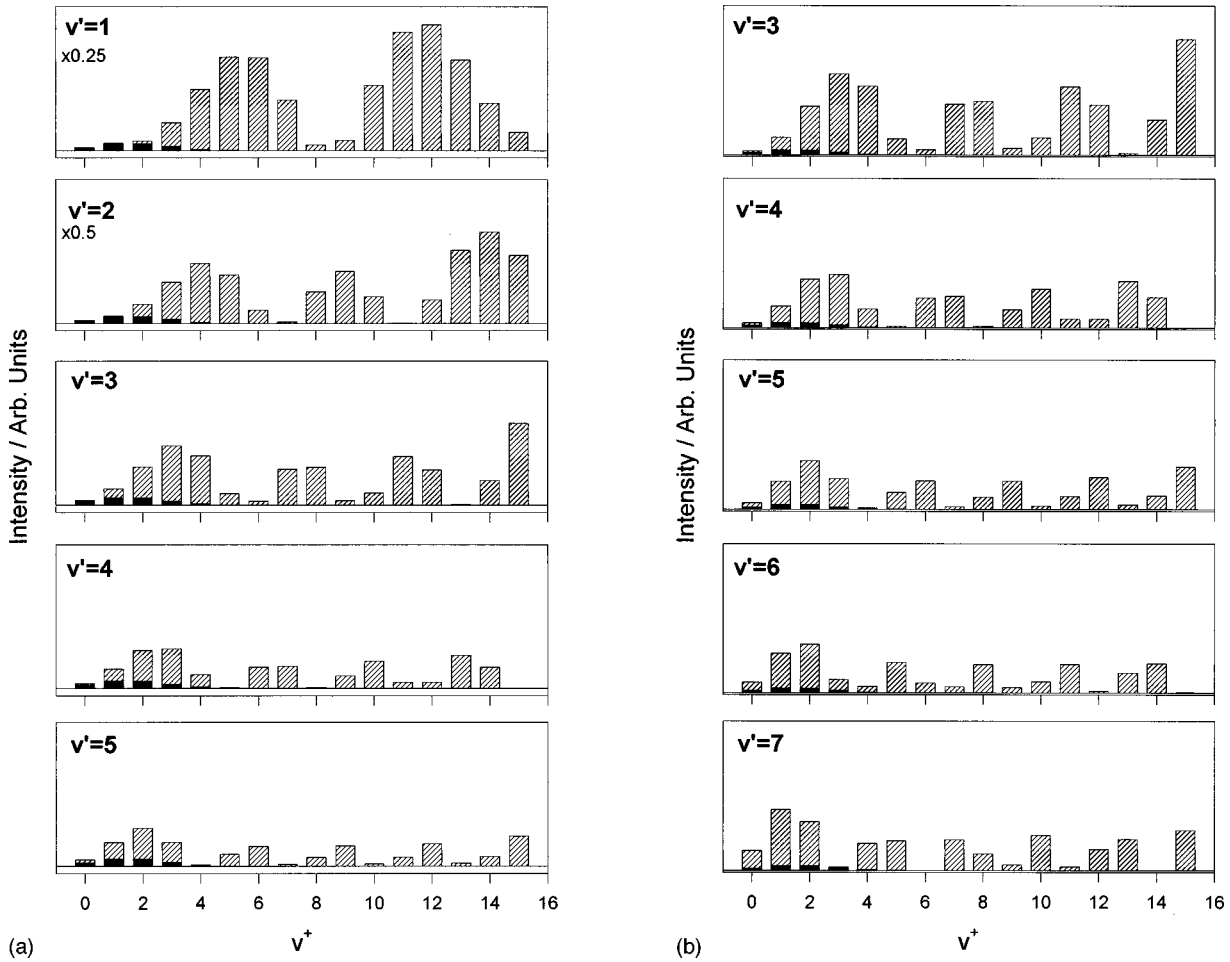

FIG. 7. Computed vibrational envelopes for the first photoelectron band of $O_2(a\ ^1\Delta_g)$, which include the direct and autoionization contributions, at photon energies of (a) 14.11 eV and (b) 14.37 eV (see the text for further details). The hatched areas represent the autoionization contributions and the solid areas the direct contributions.

The $O_2(a\ ^1\Delta_g)$ spectra in Figs. 5 and 6 may be considered as arising from two contributions, one from direct photoionization and the other from autoionization from the resonant Rydberg state. Each of these processes will have an associated Franck–Condon envelope for population of the $O_2^+(X\ ^2\Pi_g)$ state; accurate knowledge of the autoionization linewidth, Γ, and the Fano shape parameter, q, is required to allow the two envelopes to be scaled to simulate the entire resonant photoelectron spectrum.[34] However, as these parameters are not known a more empirical approach was taken. By using the intensity of the CIS background in Fig. 4 as the intensity of the direct photoionization contribution and the band intensity in Fig. 4 on a resonance as the autoionization contribution (i.e., the intensity at bands *A* or *B* in Fig. 4), the respective Franck–Condon envelopes were scaled and summed to yield a calculated photoelectron spectrum at each resonant photon energy. The vibrational component intensities obtained from this procedure are displayed as solid circles in Figs. 5 and 6, where the resonant states were assumed to be $p\ ^1\Phi_u$, $v'=3$ and $p\ ^1\Phi_u$, $v'=5$, respectively. As can be seen the agreement between the experimental and simulated envelopes is good. Computed photoelectron vibrational envelopes at $h\nu=14.11$ and 14.37 eV, which include both the direct and autoionization contributions, from selected vibrational levels of the $p\ ^1\Phi_u$, v' state, with $v'=1$, 2, 3, 4, 5, and 6, are shown in Figs. 7(a) and 7(b), respectively. Comparison of the experimental $O_2(a\ ^1\Delta_g)$ vibrational envelope in Fig. 5 (at $h\nu=14.11$ eV) with the computed envelopes, only shows good agreement for $v'=3$ [in Fig. 7(a)]. A similar comparison of Fig. 6 (at $h\nu=14.37$ eV) with Fig. 7(b) only shows good agreement for $v'=5$ confirming the vibrational numbering of the resonance levels known from the vuv absorption study[24] and shown in Fig. 4.

The success of these Franck–Condon calculations in this and previous work on autoionization of $O_2(X\ ^3\Sigma_g^-)$[35] implies that the characteristics of the resonances, in terms of autoionization linewidth, Γ, and shape parameter, q, are not important in cases where q is large, as is almost certainly the case for the resonances shown in Fig. 4, in controlling ionic vibrational level populations produced by autoionization and direct ionization.

The perturbing states responsible for the vibrationally dependent predissociation that occurs in the $p\ ^1\Phi_u$ state and competes with autoionization to the ground ionic state are not established although two dissociative $^1\Delta_u$ states and one dissociative $^1\Phi_u$ state have been proposed to cross the $p^1\Phi_u$ state.[24] Clearly further experimental and theoretical work is

needed to establish the exact positions of these curves, the extent of their interaction with the $p\,^1\Phi_u$ state, and the nature of the observed vibrationally dependent predissociation.

In summary, two strong resonances have been observed in the CIS spectra recorded for $O_2(a\ ^1\Delta_g)$. At these photon energies there is an enhancement in the photoionization cross section of $O_2(a\ ^1\Delta_g)$ and photoelectron spectra recorded at these energies allow extra vibrational structure to be obtained. At $h\nu = 14.37$ eV, the $O_2(a\ ^1\Delta_g)$ features are comparable in intensity with the $O_2(X\ ^3\Sigma_g^-)$ photoelectron features (see Fig. 6) even though the partial pressure ratio is $\approx$1:7. This implies that the $O_2(a\ ^1\Delta_g)$ photoionization cross section is nearly an order of magnitude greater than the $O_2(X\ ^3\Sigma_g^-)$ photoionization cross section at this photon energy. Also, the band associated with the $O^+(^4S) \leftarrow O(^3P)$ ionization at 13.61 eV is much more intense in Fig. 5 than Fig. 6. This is because the photon energy used for Fig. 5, 14.11 eV, corresponds to a known $O^* \leftarrow O$ resonance ($a\ ^3P \leftarrow ^3P$ transition) above the first ionization threshold of oxygen atoms.[30] This was confirmed by recording CIS spectra of the $O^+(^4S) \leftarrow O(^3P)$ band.

B. CIS spectra for $O_2^+(X\ ^2\Pi_g)\ v^+ = 0,1,2 \leftarrow O_2(a\ ^1\Delta_g)\ v'' = 0$ over the photon energy region 12.5–13.5 eV

As well as computing CIS spectra for a resonant Rydberg state with an $O_2^+(C\ ^2\Phi_u)$ core, CIS simulations were performed as have previously been described for Rydberg states with $A\ ^2\Pi_u$ and $D\ ^2\Delta_g$ ionic cores. The results of these calculations are shown in Fig. 8.

The 12.5–13.5 eV region of the experimental CIS spectrum of $O_2(a\ ^1\Delta_g)$ is shown in Fig. 9 for all four available ionic vibrational channels. Each CIS channel includes one fairly strong, broad feature (labeled *C*, *D*, *E*, and *F* in Fig. 9) as well as several weaker bands.

In this region of the CIS spectrum only Rydberg states based on the $A\ ^2\Pi_u$ core should be accessible. The Franck–Condon simulations of the CIS envelopes for such states (see Fig. 8) indicate a broad progression with the band maximum between $v' = 11$ (for $v^+ = 0$) and $v' = 6$ (for $v^+ = 3$). The $v' = 0$ component is likely to be weak for $v^+ = 0$, 1, 2, and 3 and may not be observable. The $(A\ ^2\Pi_u, 3s\sigma_g)J\ ^3\Pi_u$ Rydberg state has been well characterized by photoionization efficiency studies on $O_2(X\ ^3\Sigma_g^-)$ and has $\omega_e = 1010\ \mathrm{cm}^{-1}$, $\omega_e x_e = 3.7\ \mathrm{cm}^{-1}$, $\delta = 1.13$, and $T_0 = 13.14$ eV.[36] Assuming the $^1\Pi_u$ counterpart to have a similar quantum defect, excitation to this singlet Rydberg state from $O_2(a\ ^1\Delta_g)$ followed by autoionization to $O_2^+(X\ ^2\Pi_g)$ would be observed in the region above 12.2 eV. A number of weaker features in Fig. 9 may be components of a progression with spacings $\approx 1000\ \mathrm{cm}^{-1}$, so that it is possible that they correspond to autoionization from $(A\ ^2\Pi_u, 3s\sigma_g)^1\Pi_u$ although no positive identification of a transition to this state can be made with the rather poor signal-to-noise ratios obtained.

The stronger resonances *C*, *D*, *E*, and *F* in Fig. 9 exhibit unusual behavior. Each autoionizes preferentially to a certain v^+ level and weakly to $v^+ + 1$ with no appreciable intensity in other channels, implying good Franck–Condon overlap of each $O_2^*\ v'$ resonant level with only one v^+ level. As the vibrational quantum number in the $O_2^+(X\ ^2\Pi_g)$ state is increased by one from $v^+ = 0$, the dominant resonance moves to lower energy by about 1700 cm^{-1}. This separation is far higher than any vibrational separation in any known excited state of O_2^+, so bands *C*–*F* are unlikely to represent transitions to consecutive vibrational levels of Rydberg states built upon such cores. For example, if the O_2^* state were of $(A\ ^2\Pi_u, nl\lambda)$ character, features *C*–*F* would each have to be separated by two vibrational quanta; this seems highly implausible given that the experimental envelopes associated with bands *C*–*F* in Fig. 9 are at odds with the simulated CIS envelopes in Fig. 8.

The higher vibrational levels of $O_2^+(X\ ^2\Pi_g)$ are separated by $\approx 1700\ \mathrm{cm}^{-1}$, so bands *C*–*F* might be considered as transitions to members of Rydberg series converging to these high v^+ levels and autoionizing vibrationally. However, since the potential energy curves of the ground ionic state and Rydberg states with the same ionic core should be approximately parallel, a $\Delta v = -1$ propensity rule should apply.[37] This clearly cannot be the case for bands *C*–*F* with separations of up to 2.5 eV between the resonant features *C*–*F* and the ionization thresholds being observed in Fig. 9.

It would appear that the stronger features *C*–*F* in Fig. 9 cannot be assigned to transitions to Rydberg states built on any known states of O_2^+. Instead the presence of an autoionizing valence (or mixed Rydberg-valence) state seems more likely. The interpretation which is favored for bands *C*–*F* is that they arise from autoionization to $O_2^+(X\ ^2\Pi_g)$ from vibrational turning points on the steeply rising part of the potential of a perturbed valence state. A schematic diagram showing part of an excited state potential (obtained by joining up the solid black circles) and the $O_2^+(X\ ^2\Pi_g)$ potential, which would give rise to CIS spectra of the type shown in Fig. 9 is shown in Fig. 10. Left-hand turning points of vibrational levels in the excited state potential, denoted by the black solid circles, are accessible from $O_2(a\ ^1\Delta_g)$, $v'' = 0$ and are in this model accessed at 13.46 eV (*C*), 13.25 eV (*D*), 13.04 eV (*E*) and 12.84 eV (*F*). Further work is clearly necessary to elucidate the nature of these resonances.

C. $O_2^+(X\ ^2\Pi_g)\ v^+ \leftarrow O_2(a\ ^1\Delta_g)\ v'' = 0$ CIS spectra recorded in the photon energy region 15.5–19.0 eV

Figure 11 shows the 15.5–17.0 eV region of the $O_2^+(X\ ^2\Pi_g)\ v^+ = 1,2,3 \leftarrow O_2(a\ ^1\Delta_g)\ v'' = 0$ CIS spectra. The $v^+ = 0$ signal proved to be too weak to enable reliable spectra to be recorded and is not shown. A number of features are observed in the $v^+ = 1$, 2, and 3 spectra, many of which are reproduced in each ionic vibrational channel. The structure observed must arise from overlap of transitions to a number of Rydberg states, only one of which can be assigned with any confidence here.

The spacings between features *G*, *H*, *I*, and *J* in Fig. 11 are constant at $(950 \pm 30)\ \mathrm{cm}^{-1}$ suggesting that these features are transitions to successive vibrational members of a Rydberg state based on the ionic states $C\ ^2\Phi_u$ ($\omega_e = 1042\ \mathrm{cm}^{-1}$) or $D\ ^2\Delta_g$ ($\omega_e = 995\ \mathrm{cm}^{-1}$). (The $O_2^+ A\ ^2\Pi_u$ state is eliminated as an ionic core as it has AIE = 16.06 eV and $\omega_e = 898\ \mathrm{cm}^{-1}$). Despite the structured region observed

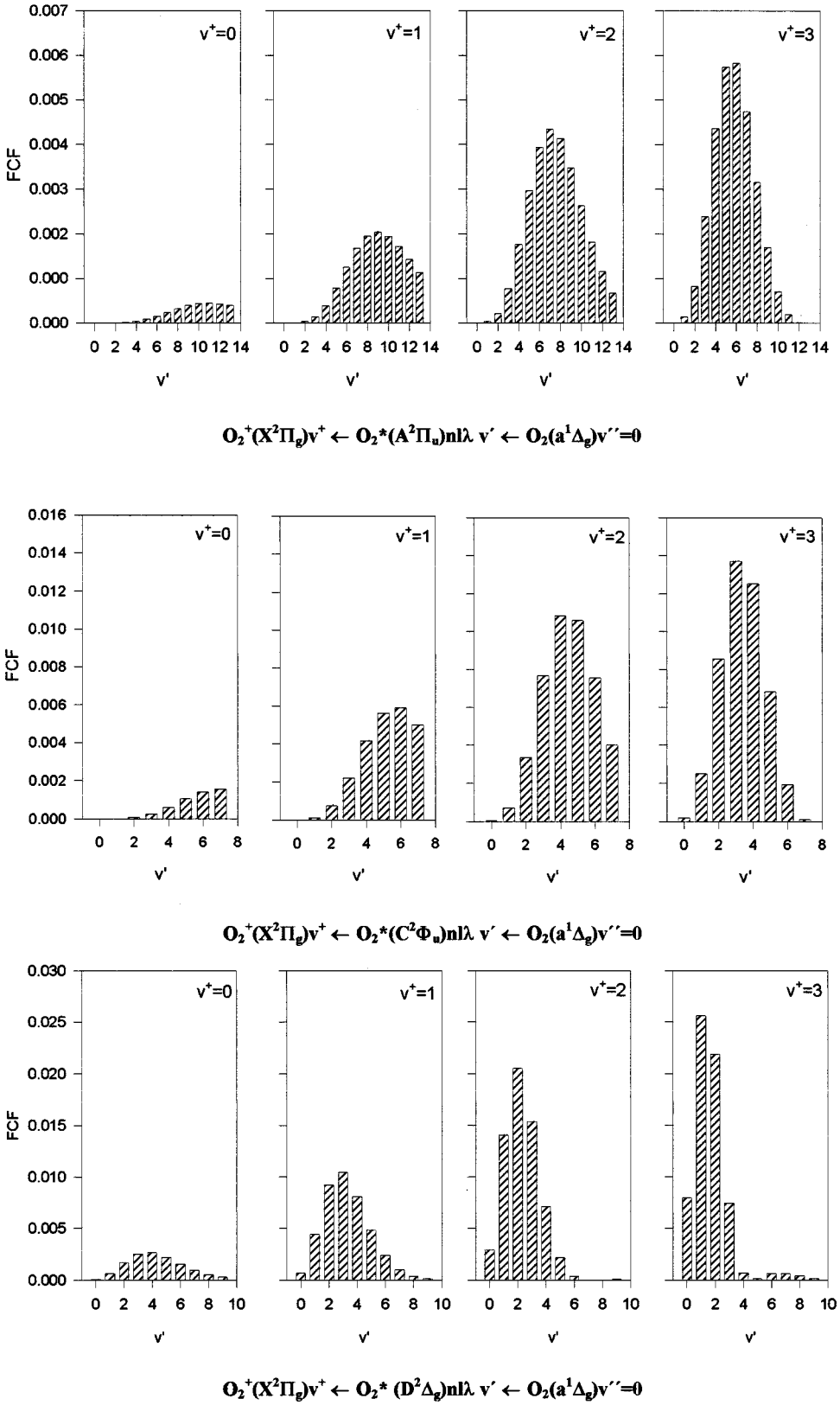

FIG. 8. Computed CIS envelopes for $O_2^+(X\ ^2\Pi_g)v^+ \overset{(b)}{\leftarrow} O_2^*$, $v' \overset{(a)}{\leftarrow} O_2(a\ ^1\Delta_g)$, $v''=0$, where O_2^* represents a Rydberg state with an ionic core chosen as follows: (a) $O_2^+(A\ ^2\Pi_u)$, (b) $O_2^+(C\ ^2\Phi_u)$, and (c) $O_2^+(D\ ^2\Delta_g)$. The CIS envelopes were obtained by multiplying the Franck–Condon factors of steps (a) and (b) together (see the text for further details).

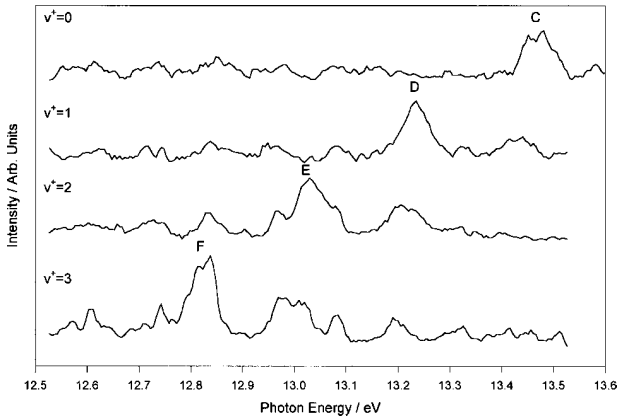

FIG. 9. $O_2^+(X\ ^2\Pi_g)v^+ \leftarrow O_2(a\ ^1\Delta_g)v''=0$ CIS spectra recorded in the photon energy region 12.5–13.6 eV, for $v^+=0$, 1, 2, and 3.

to lower energy of band *G* in Fig. 11, no clear component is observed at the correct spacing below this feature to extend the series labeled *G*–*J* to lower energy.

Assuming that feature *G* (at 16.07 eV) corresponds to $v'=0$ in the upper state then effective quantum numbers of 3.07 and 2.23 are calculated for Rydberg states based on

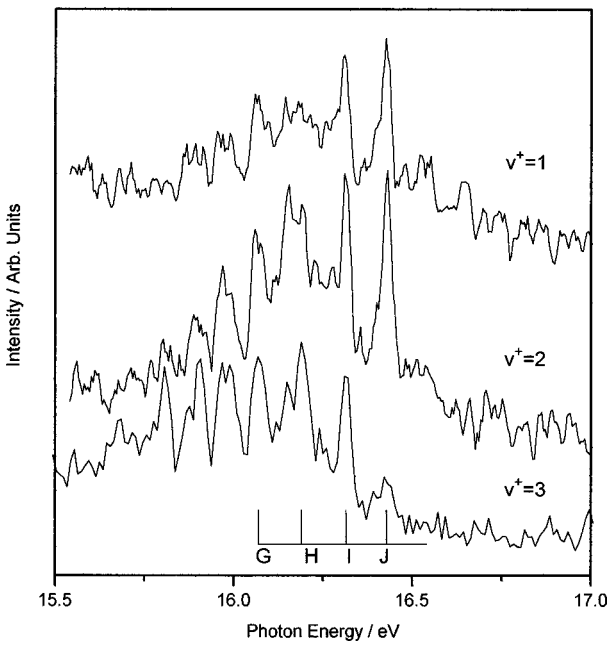

FIG. 11. $O_2^+(X\ ^2\Pi_g)$, $v^+ \leftarrow O_2(a\ ^1\Delta_g)v''=0$ CIS spectra recorded in the photon energy region 15.5–17.0 eV, for $v^+=1$, 2, and 3.

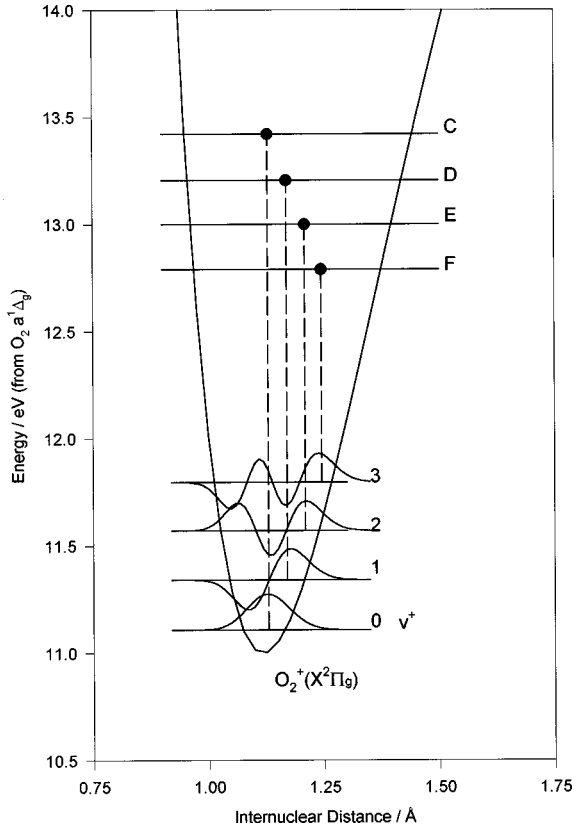

FIG. 10. A schematic diagram showing part of an excited state potential (obtained by joining up the solid circles) and the $O_2^+(X\ ^2\Pi_g)$ potential which would give rise to CIS spectra of the type shown in Fig. 9. The positions of resonances *C*, *D*, *E*, and *F* (shown in Fig. 9) from $O_2(a\ ^1\Delta_g)v''=0$ are marked on the diagram. Left-hand turning points (marked by the solid circles) of vibrational levels in the excited state, denoted *C*, *D*, *E*, and *F*, are all accessible from $O_2(a\ ^1\Delta_g)$, $v''=0$ ($r_e=1.2156$ Å) (Ref. 33) and are in this model accessed at photon energies of 13.46 eV (*C*), 13.25 eV (*D*), 13.04 eV (*E*), and 12.84 eV (*F*).

$C\ ^2\Phi_u$ and $D\ ^2\Delta_g$ ionic cores, from the known adiabatic ionization energies to the *C* and *D* ionic states from $O_2(a\ ^1\Delta_g)$. These effective quantum numbers would be consistent with excitation to $(C\ ^2\Phi_u,4s\sigma_g)\ ^1\Phi_u$ or $(D\ ^2\Delta_g,3p\pi_u)\ ^1\Pi_u$, $^1\Phi_u$ states.[32] The latter assignment, corresponding to a $(D\ ^2\Delta_g,3p\pi_u)$ ($\delta=0.77$) state, is preferred since it has a lower value of *n* than that of the *C* state assignment and the observed vibrational spacings in the band labeled *G*–*J* in Fig. 11 are closer to those of the *D* ionic state. This assignment is supported by the CIS simulations shown in Fig. 8. These calculations indicate that the CIS envelope should peak at lower v' values as v^+ increases, as is observed, and that for a Rydberg state with a $D\ ^2\Delta_g$ ionic core, the $v'=3$ signal should be much weaker in the $v^+=3$ CIS spectrum than in the $v^+=2$ CIS spectrum. This is in agreement with a $(D\ ^2\Delta_g,3p\pi_u)$ assignment in which feature *J* corresponds to $v'=3$. CIS calculations for a Rydberg state based on a $C\ ^2\Phi_u$ ionic core suggest the opposite trend, i.e., that $v'=3$ autoionizes more strongly to $v^+=3$ than $v^+=2$, contrary to the experimental observation. The observed intensity of the $v'=0$ component, feature *G* in Fig. 11, is greater than that expected from the CIS simulations but this is understandable as it is overlapped by an unassigned band to low photon energies. Although more features are observed in Fig. 11, no other vibrational progressions can be unambiguously identified.

In summary, bands *G*–*J* in Fig. 11 are assigned to excitation to a $(D\ ^2\Delta_g,3p\pi_u)$ state even though the $(C\ ^2\Phi_u,4s\sigma_g)\ ^1\Phi_u$ state is expected in this region and the transition to the $(C\ ^2\Phi_u,3s\sigma_g)\ ^1\Phi_u$ state at lower energy is particularly intense (Fig. 4). This assignment means that a broad weak band centered at ≈17.75 eV (see Fig. 3) in both the $v^+=1$ and $v^+=2$ CIS spectra can be assigned to the excitation $O_2^*\ (D\ ^2\Delta_g,4p\pi_u) \leftarrow O_2(a\ ^1\Delta_g)$.

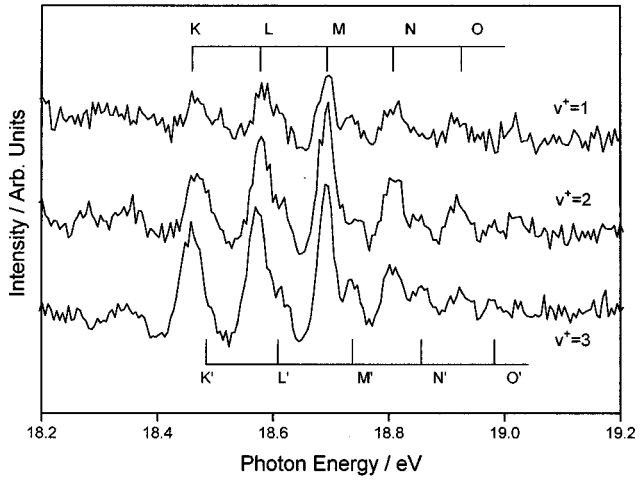

FIG. 12. $O_2^+(X\ ^2\Pi_g)v^+ \leftarrow O_2(a\ ^1\Delta_g)v''=0$ CIS spectra recorded in the photon energy region 18.2–19.2 eV, for $v^+=1$, 2, and 3.

The final photon energy region in which discrete structure was observed was 18.2–19.2 eV. CIS spectra recorded for $O_2^+(X\ ^2\Pi_g)$ $v^+=1$, 2, and 3 over this range are shown in Fig. 12. Once again the $v^+=0$ signal proved to be too weak to record reliable spectra. Relatively strong features labeled *K*, *L*, *M*, *N*, and *O* form a clear vibrational progression with a mean spacing of (940 ± 30) cm^{-1}. A second, weaker progression which partly overlaps the first (labeled K', L', M', N', and O' in Fig. 12), can also be identified and has a mean vibrational spacing of (1000 ± 30) cm^{-1}.

The only well-characterized state of O_2^+ accessible from $O_2(a\ ^1\Delta_g)$ above 18.0 eV photon energy is the $D\ ^2\Delta_g$ state with an adiabatic ionization energy of 18.81 eV from $O_2(a\ ^1\Delta_g)$.[14,15,31] Assuming feature *K* (at 18.46 eV) to correspond to the first component of a vibrational progression, the effective principal quantum number of the associated Rydberg state based on a $D\ ^2\Delta_g$ ionic core is calculated to be 6.23, suggesting a $(D\ ^2\Delta_g, 7p\pi)$ $(\delta=0.77)$ assignment.[32] However, the high value of *n* and the absence of any experimental evidence of members of this series with $n=5$ or 6 at lower photon energies (although the $3p$ and $4p$ components have been observed) does not support this interpretation. Also, the CIS simulations of Fig. 8 are not consistent with this assignment as, if the ionic core is $D\ ^2\Delta_g$, the CIS vibrational profiles are calculated to change with v^+, in contrast to the very unusual experimental observation that the CIS vibrational profile is essentially the same in all v^+ channels.

An ionic state of unknown symmetry has been observed by Baltzer *et al.*[3] as a weak progression between the vibrational components of the $O_2^+(B\ ^2\Sigma_g^-) \leftarrow O_2(X\ ^3\Sigma_g^-)$ band in the high-resolution photoelectron spectrum of ground-state oxygen. Baltzer *et al.*[3] analyzed the vibrational structure in the observed photoelectron band to yield $\omega_e=830\ cm^{-1}$ in the ionic state and suggested that this state might be a $^2\Delta_g$ state. The adiabatic ionization energy to this state is 20.35 eV, from $O_2(X\ ^3\Sigma_g^-)$, and 19.37 eV from $O_2(a\ ^1\Delta_g)$, although it is not known if it is accessible from $O_2(a\ ^1\Delta_g)$. However, if the feature *K* in Fig. 12 is the first component of a transition to a Rydberg state with this ionic core, then an effective principal quantum number of 3.87 can be derived for the excited Rydberg state. This may correspond to a state with the excited electron in a $4d\sigma_g$, $4d\pi_g$ $(\delta=0.13)$ or $5s\sigma_g$ $(\delta=1.13)$ Rydberg orbital, any one of which is also plausible for the state associated with the second vibrational series (K',L',M',N',O'). However, for this ionic state to be accessible from both the $X\ ^3\Sigma_g^-$ and $a\ ^1\Delta_g$ neutral states, it must have $^2\Pi_u$ or $^2\Pi_g$ symmetry contrary to the suggestion of Balzer *et al.*[3] that it is a $^2\Delta_g$ state. In summary, the two vibrational progressions observed in the CIS spectra of $O_2(a\ ^1\Delta_g)$ recorded in the 18.2–19.2 eV region must remain unassigned until the ionic states accessible from $O_2(a\ ^1\Delta_g)$ in the ionization energy region 20–22 eV have been fully characterized.

In conclusion, the variable photon energy facility of a synchrotron source has enabled CIS spectra of $O_2(a\ ^1\Delta_g)$ to be recorded and hence has allowed highly excited singlet states of $O_2(a\ ^1\Delta_g)$ above the first ionization threshold to be investigated. This has established wavelengths in the vacuum ultraviolet region in which the photoionization cross section of this atmospherically important species is enhanced. The largest increase in photoionization cross section occurs at photon energies of 14.11 and 14.37 eV. The excited Rydberg state associated with these resonances has been assigned and photoelectron spectra of the first band of $O_2(a\ ^1\Delta_g)$ recorded at these resonant energies exhibit extended vibrational structure with 16 vibrational components being observed compared to only four components observed in the off-resonance spectra. Suggestions are made for assignment of the weaker structure observed in the CIS spectra. This work is currently being extended to other short-lived molecules where extra vibrational structure in a photoelectron band should be very useful in helping to characterize the associated ionic state.

ACKNOWLEDGMENTS

The authors thank the EPSRC, NERC, and the Leverhulme Trust for financial support of this work. T.G.W. thanks the EPSRC for the award of an Advanced Fellowship and S.S. gratefully acknowledges support from MURST (Italy).

[1] P. M. Dehmer and W. A. Chupka, J. Chem. Phys. **62**, 4525 (1975).
[2] O. Edqvist, E. Lindolm, L. E. Selin, and L. Asbrink, Phys. Scr. **1**, 25 (1970).
[3] P. Baltzer, B. Wannberg, L. Karlsson, M. Carlsson Gothe, and M. Larsson, Phys. Rev. A **45**, 4374 (1992).
[4] K. Ellis, R. I. Hall, L. Avaldi, G. Dawber, A. McConkey, L. Andric, and G. C. King, J. Phys. B **27**, 3415 (1994).
[5] F. Merkt and P. M. Guyon, J. Phys. Chem. **99**, 15775 (1995).
[6] W. Kong and J. W. Hepburn, Int. J. Mass Spectrom. Ion Processes **159**, 27 (1996).
[7] T. Akahori, Y. Morioka, T. Tanaka, H. Yoshii, T. Hayaishi, and K. Ito, J. Chem. Phys. **107**, 4875 (1997).
[8] G. Marston, Chem. Soc. Rev. , 33 (1996).
[9] D. M. Hunter and M. B. McElroy, J. Geophys. Res. **73**, 2421 (1968).
[10] W. F. J. Evans, D. M. Hunter, E. J. Llewellyn, and A. Vallance-Jones, J. Geophys. Res. **73**, 2885 (1968).
[11] R. P. Wayne, Adv. Photochem. **7**, 311 (1969).
[12] E. E. Ferguson and F. C. Fehsenfeld, J. Geophys. Res. **74**, 5743 (1969).
[13] E. E. Ferguson, F. C. Fehsenfeld, and D. L. Albritton, in *Gas-Phase Ion Chemistry*, edited by M. T. Bowers (Academic, New York, 1979), Vol. 1.

[14] N. Jonathan, A. Morris, M. Okuda, K. J. Ross, and D. J. Smith, J. Chem. Soc., Faraday Trans. 2 **70**, 1810 (1974).
[15] H. van Lonkhuyzen and C. A. de Lange, J. Electron Spectrosc. Relat. Phenom. **27**, 255 (1982).
[16] H. Park, L. Li, and W. A. Chupka, J. Chem. Phys. **92**, 61 (1990).
[17] H. Park, L. Li, and W. A. Chupka, Chem. Phys. Lett. **162**, 317 (1989).
[18] R. J. Yokelson, R. J. Lipert, and W. A. Chupka, J. Chem. Phys. **97**, 6144 (1992); **97**, 6153 (1992).
[19] A. Sur, R. S. Friedman, and P. J. Miller, J. Chem. Phys. **94**, 1705 (1991).
[20] R. D. Johnson, G. R. Long, and J. W. Hudgens, J. Chem. Phys. **87**, 1977 (1987).
[21] R. Ogorzalek Loo, W. J. Marinelli, P. L. Houston, S. Arepelli, J. R. Wisenfeld, and R. W. Field, J. Chem. Phys. **91**, 5185 (1989).
[22] R. E. Huffman, D. E. Paulsen, J. C. Larrabee, and R. B. Cairns, J. Geophys. Res. **76**, 1028 (1971).
[23] R. J. Collins, D. Husain, and R. J. Donovan, J. Chem. Soc., Faraday Trans. 2 **69**, 145 (1973).
[24] D. H. Katayama, R. E. Huffman, and Y. Tanaka, J. Chem. Phys. **62**, 2929 (1975).
[25] R. E. Huffman, J. C. Larrabee, and Y. Tanaka, J. Chem. Phys. **46**, 2231 (1967).
[26] D. H. Katayama, S. Ogawa, M. Ogawa, and T. Tanaka, J. Chem. Phys. **67**, 2132 (1977).
[27] J. M. Dyke, D. Haggerston, A. Morris, S. Stranges, J. B. West, T. G. Wright, and A. E. Wright, J. Chem. Phys. **106**, 821 (1997).
[28] J. M. Dyke, S. D. Gamblin, D. Haggerston, A. Morris, S. Stranges, J. B. West, T. G. Wright, and A. E. Wright, J. Chem. Phys. **108**, 6258 (1998).
[29] W. J. van der Meer, P. van der Meulen, M. Volmer, and C. A. de Lange, Chem. Phys. **126**, 385 (1988).
[30] C. E. Moore, *Atomic Energy Levels*, *Volume 1*, Circular of the National Bureau of Standards 467, 1949 (U.S. Govt. Printing Office, Washington D.C.).
[31] H. van Lonkhuyzen, Ph.D thesis, Free University, Amsterdam, 1984.
[32] E. Lindolm, Ark. Fys. **40**, 117 (1969); C. Y. R. Wu, J. Quant. Spectrosc. Radiat. Transf. **37**, 1 (1987).
[33] K. P. Huber and G. Herzberg, *Molecular Spectra and Molecular Structure IV Constants of Diatomic Molecules* (van Nostrand Reinhold, New York, 1979).
[34] A. L. Smith, Philos. Trans. R. Soc. London, Ser. A **268**, 169 (1970).
[35] J. H. D. Eland, J. Chem. Phys. **72**, 6015 (1980).
[36] E. Nishitani, I. Tanaka, K. Tanaka, T. Kato, and I. Koyano, J. Chem. Phys. **81**, 3429 (1984).
[37] J. Berkowitz, *Photoabsorption, Photoionization and Photoelectron Spectroscopy* (Academic, New York, 1979); J. Berkowitz and W. A. Chupka, J. Chem. Phys. **51**, 2341 (1969).